Universal Response of Single-Wall Carbon Nanotubes to Radial Compression

A. P. M. Barboza, H. Chacham,* and B. R. A. Neves†

Departamento de Física, ICEX, Universidade Federal de Minas Gerais, CP 702, 30123-970, Belo Horizonte, MG, Brazil
(Received 2 October 2008; published 14 January 2009)

The mechanical response of single-wall carbon nanotubes to radial compression is investigated via atomic force microscopy (AFM). We find that the force F applied by an AFM tip (with radius R) onto a nanotube (with diameter d), rescaled through the quantity $Fd^{3/2}(2R)^{-1/2}$, falls into a universal curve as a function of the compressive strain. Such universality is reproduced analytically in a model where the graphene bending modulus is the only fitting parameter. The application of this model to the radial Young's modulus E_r leads to a further universal-type behavior which explains the large variations of nanotube E_r reported in the literature.

DOI: 10.1103/PhysRevLett.102.025501 PACS numbers: 62.25.−g, 61.48.De, 68.37.Ps, 81.07.De

Since the early 1990s, the electronic and structural properties of single-wall carbon nanotubes (SWNTs) have been thoroughly investigated and some applications of those properties have been proposed [1–18]. Regarding SWNT mechanical properties, most of the attention has been given to their large resistance to axial tension [1,3,4,6], even though several electromechanical effects have been observed on radially compressed SWNTs [14–18]. A universal and consistent understanding of the mechanical properties of SWNT under radial compression is also still missing: for instance, reported values of the radial Young's modulus E_r vary by up to 3 orders of magnitude [5,7–13]. The present work brings a unifying picture to the process of radial compression (deformation) of SWNTs, where experimental data are analyzed through a rescaling model yielding a universal-type behavior. Specifically, we find that the quantity $Fd^{3/2}(2R)^{-1/2}$, where F is the force applied by an atomic force microscopy (AFM) tip (with radius R) and d is the SWNT diameter, is a universal function of the compressive strain. The application of the same model to the radial Young's modulus E_r leads to a further universal-type behavior that explains the large variations of the SWNTs E_r reported in the literature [5,7–13]. Finally, the implications of such universal-type behavior to nanometrology are briefly discussed.

Sample growth was accomplished on a 100 nm-thick SiO_x layer on top of a Si substrate using a chemical vapor deposition procedure which selectively produces SWNTs [19]. Several of these SWNTs were investigated by scanning probe microscopy (SPM) (Nanoscope IV MultiMode SPM, from Veeco Instruments). The SPM measurements were carried out in air (in most cases), or under dry nitrogen atmospheres (in some cases) with the help of a home-made environmental control chamber. Silicon and silicon nitride cantilevers with nominal spring constants k from 0.08 to 0.25 N/m, nominal radii of curvature $R \approx 30$ nm and resonant frequencies ω_0 from 20 to 40 kHz were employed throughout this work for AFM imaging (contact and intermittent contact modes) and compression (deformation) experiments. More accurate estimations of k and R were carried out by the use of the Sader's method [20] and by the analysis of SWNT images, respectively [10,21].

Figure 1(a) and the inset of Fig. 1(b) illustrate the experimental procedure employed to acquire compression (deformation) data throughout this work. Instead of using a nanoindentation protocol, which requires both sub-nm precision and stability on the AFM tip positioning, employed in all experimental works published so far [10,12,14–16], SWNTs were simply imaged in AFM contact mode, as seen in Fig. 1(a). During image acquisition, the SWNT axis is kept perpendicular to the fast scan (horizontal) direction while the slow scan (vertical) axis is disabled; i.e., the same region of the SWNT is probed in the entire image. Concomitantly, the SWNT compression is varied through changes on the AFM tip normal force F at finite time intervals. Therefore, beginning at the top of Fig. 1(a), the compression force is sequentially increased (downward) from 2 up to 25 nN. In such a way, the radial deformation of each nanotube due to a given tip compression force can be determined straightforwardly through the apparent height h of each nanotube in the AFM image [see inset of Fig. 1(b)]. The plot in Fig. 1(b) summarizes this new methodology showing the observed height h of several SWNTs as a function of the compression force F exerted by the AFM tip. It is clear in Fig. 1(b) that all SWNTs are deformed by the tip during the imaging process, with a pronounced decrease of SWNT height as the compression force is increased. A plot of the compressive force F versus SWNT deformation is shown in Fig. 2(a) [22]. Inspecting Fig. 2(a), apart from the obvious increase of measured deformation with the applied force, no other universal behavior can be inferred from its scattered data. Even a plot of F versus radial strain (data not shown) for each SWNT does not provide any indication of a unifying picture.

The standard methodology used in experimental works dealing with radial deformation of nanotubes [9,10,12] is based on the Hertzian model (and some variations) of bulk

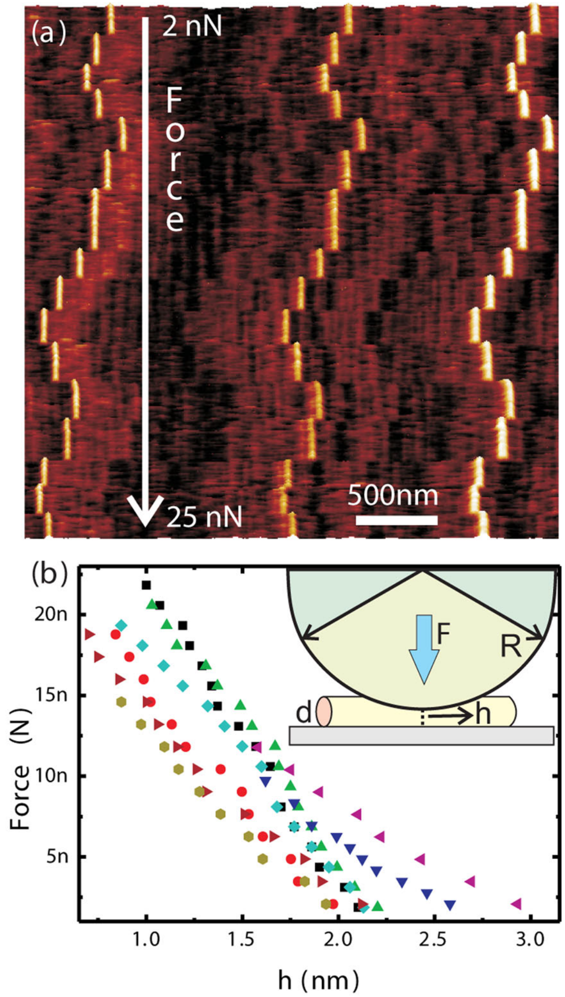

FIG. 1 (color online). (a) AFM images showing the same region of three SWNTs. From top to bottom, the compressive force exerted by the tip sequentially increases from 2 up to 25 nN. At each force variation step, the sample position is intentionally shifted laterally in order to distinguish each compression regime. (b) Observed height h of several SWNTs versus compressive force F (different AFM tips were used to collect these data). Inset: schematic drawing identifying all relevant parameters: the compressive force F, the AFM tip radius R, the SWNT diameter d, and its measured height h.

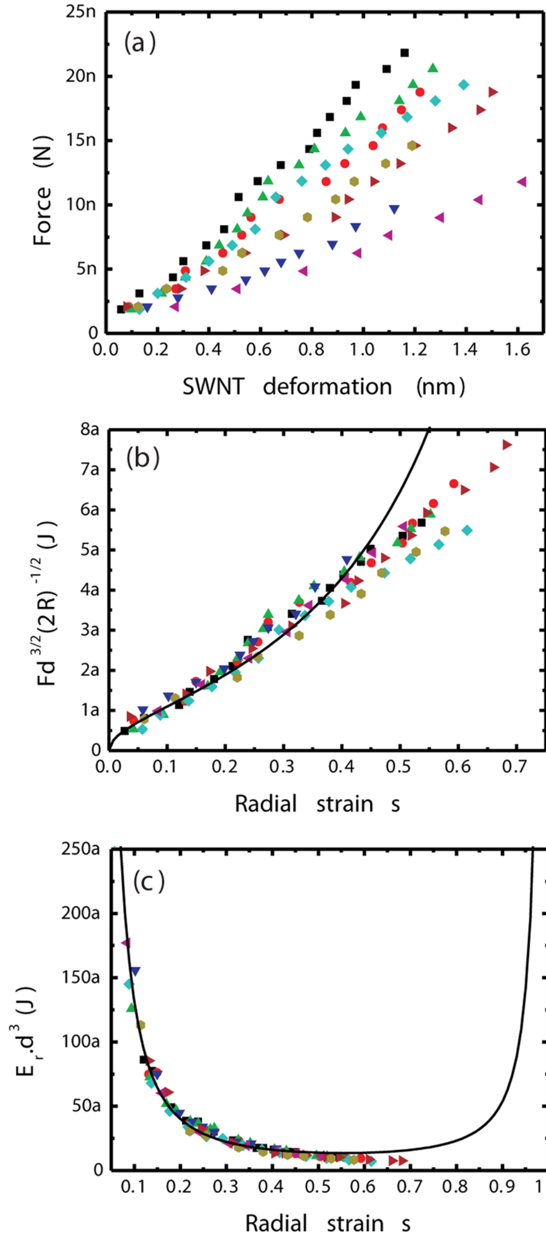

FIG. 2 (color online). (a) Applied compressive force F versus the observed deformation of several SWNTs. (b) Dependence of the quantity $Fd^{3/2}(2R)^{-1/2}$ on the radial strain $s = 1 - h/d$. The line corresponds to Eq. (1) with $a = 1.2 \times 10^{-18}$ J. (c) Dependence of the quantity $E_r(s)d^3$ (where E_r is the radial Young's modulus) on s for several SWNTs. The line corresponds to Eq. (2) with the same a as above.

deformation under an applied load [23]. The Hertzian model, however, considers a constant value of the radial Young's modulus E_r. This assumption is unrealistic for SWNTs: in this case, as we will show below, E_r is a strongly varying function of the radial strain s. Therefore, we developed a new model that does not assume a constant E_r, as follows.

As a starting point of the model, we consider the results of first-principles calculations that predict that the compressive force per unit length on a SWNT, F/l, as a function of its local height, y, can be approximated by $F/l = a/y^2$ if $y < d$, where d is the original nanotube diameter [18,24]. For $y > d$ we assume that the force is null [25]. These results are consistent with a continuum model [24], and the constant a can be related to the graphene bending modulus β [28] through $a = \pi\beta\sigma$, where σ is the area density of carbon atoms in graphene. The inset of Fig. 1(b) shows that, during the AFM imaging process, the nanotube height y varies from a minimal value h, the measured height, up to the maximal value d, following the AFM tip morphology. Therefore, the total force F is calculated through integration over the AFM tip-SWNT contact length, resulting in

$$F = (2R/d^3)^{1/2} \frac{a}{(1-s)^{3/2}} \left[\sqrt{2s + s^2} + tg^{-1}\left(\sqrt{\frac{s}{1-s}} \right) \right], \tag{1}$$

where R is the AFM tip radius [see inset of Fig. 1(b)] and s is the radial strain [$s = (d - h)/d$]. Equation (1) shows that the rescaled quantity $Fd^{3/2}(2R)^{-1/2}$, in energy units, should be universal to any SWNT, depending only on its radial strain s and the (universal) constant a.

In order to test the scaling property predicted by Eq. (1), we plot in Fig. 2(b) the rescaled quantity $Fd^{3/2}(2R)^{-1/2}$ as a function of the strain s, for the same data of Fig. 2(a). The universal-type behavior is evident in Fig. 2(b), as the data for all nanotubes fall into a single curve. Moreover, the analytical result for F from Eq. (1) is also plotted in Fig. 2(b) (black line) where we take the value of $a = 1.2 \times 10^{-18}$ J from the *ab initio* calculations of Ref. [18]. The agreement between theory—which has a single parameter obtained from first principles—and experiment is remarkable for moderate SWNT strain ($s < 0.5$). For larger values of strain the universal-type behavior seems to hold for the experimental data, but it is not well described by the theoretical model of Eq. (1) anymore.

The strong correlation between experimental data and theory in Fig. 2(b) for small values of strain can also be used to estimate the value of a, and consequently the graphene bending modulus β. A nonlinear fitting of the experimental data of Fig. 2(b) for $s < 0.25$ with Eq. (1) results in $a = (1.26 \pm 0.02) \times 10^{-18}$ J, or, equivalently, in $\beta = a/(\pi\sigma) = (66 \pm 1)$ meV nm^2, where we used an area density of carbon atoms in graphene $\sigma = 38.12$ nm^{-2}. This is in good agreement with another recent estimate of β [(55 ± 10) meV nm^2] from AFM measurements in double-wall nanotubes [28].

The model described by Eq. (1) can also be applied to the analysis of SWNT radial Young's modulus E_r. From the definition, $E_r(s) = F/(As)$, where A is the tip-nanotube contact area [29]. Therefore, it follows that

$$E_r(s) = \frac{6a}{5\pi d^3 s^{5/2}(1-s)^{3/2}} \left[\sqrt{2s + s^2} + tg^{-1}\left(\sqrt{\frac{s}{1-s}} \right) \right]. \tag{2}$$

Equation (2) leads to three interesting conclusions: (i) The radial Young's modulus of a SWNT is not a constant, but it depends on the nanotube deformation (strain s). Indeed, Eq. (2) indicates arbitrarily large E_r values for either very small or very large SWNT strain, and modest values for moderate strain. (ii) Keeping the strain fixed, the radial Young's modulus follows a $1/d^3$ behavior (in previous works, there has been some debate whether E_r varies with $1/d$, $1/d^2$, or $1/d^3$ [5,7–13]); (iii) The quantity $E_r(s)d^3$ should also present a universal-type behavior, depending only on SWNT strain. In order to verify such behavior, a "semiexperimental" radial Young's modulus $E_r^{\mathrm{Exp}}(s)$ was evaluated using its definition above [$E_r^{\mathrm{Exp}}(s) = F^{\mathrm{Exp}}/(As)$, where F^{Exp} is the experimental force data] and the product $E_r(s)d^3$ is shown in Fig. 2(c) for all SWNTs. Again, a universal-type behavior is evident in this figure, where the black line represents the theory from Eq. (2) (also calculated using $a = 1.2 \times 10^{-18}$ J, from Ref. [18]). Once again, the agreement between experimental data and theory is evident up to moderate SWNT strain values. It is also noteworthy that both the results in Fig. 2(c) and the conclusion (i) above explained the large variation on the measured E_r values reported in the literature, from a few GPa range up to more than a thousand GPa [5,7–13]. These values should be larger for very small, or very large, SWNT deformations, and smaller for moderate deformations, which again is in agreement with reported values in the literature [10,12].

Nanometrology is certainly one of the most difficult, but necessary, challenges of nanotechnology. The universal-type behavior of SWNT under radial compression described in this work may represent a step forward in this path. Consider, for example, the quantity $Fd^{3/2}(2R)^{-1/2}$, which is a function of SWNT strain only and, thus, should be constant for a fixed strain value. It correlates three important parameters at the nanoscale: force, in the nano-Newton range, and both SWNT and AFM tip diameters, also in the nanometer range. In other words, for a given strain, if two of those quantities are known, the third can be determined. For instance, if the SWNT diameter is precisely determined via Raman spectroscopy [1] and the AFM tip geometry is well defined, or determined via high-resolution electron microscopy, the radial compression experiment can be seen as a gauge for precise force determination at the nanoscale. Alternatively, if force and tip geometry are known, this methodology could be used for precise determination of SWNT diameter. As an illustration of the interplay among these quantities and correspondence between theory and experiment, Fig. 3 shows the experimental applied compressive force F versus the rescaling quantity $(R/d^3)^{1/2}$ for two specific values of strain [$s = 0.25$ (squares) and $s = 0.15$ (circles)]. The lines in Fig. 3 are linear fits to the experimental data and their angular coefficients α are $\alpha_{0.25} = (3.9 \pm 0.4)$ and $\alpha_{0.15} = (1.8 \pm 0.2)$, respectively. For these strain values, the theory [through Eq. (1)] predicts $\alpha_{0.25} = 3.4$ and $\alpha_{0.15} = 2.0$, indicating, once more, a good agreement between experiment and theory. Therefore, the plot in Fig. 3 could be employed for accurate determination, or prediction, of the values of any of the three parameters (F, d, and R), if two of them are known, in a similar way of Kataura plots, which correlate SWNT transition energy, its diameter, and Raman shift [1].

In conclusion, this work has shown that through an appropriate rescaling procedure, SWNTs present a

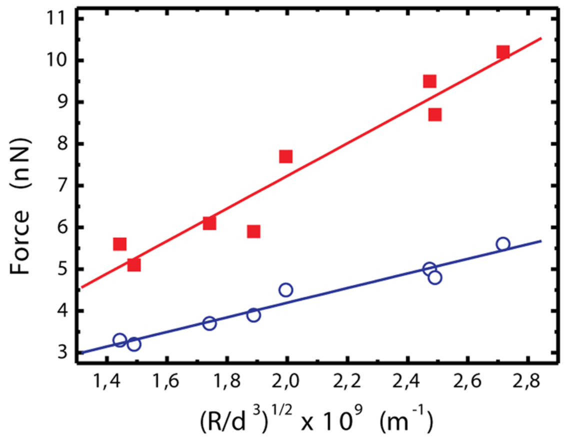

FIG. 3 (color online). Experimental compressive force versus the rescaling factor $(R/d^3)^{1/2}$ for two specific radial strain values, $s = 0.15$ (circles) and $s = 0.25$ (squares). The lines are best linear fits.

universal-type behavior when radially compressed by an AFM tip. The developed experimental procedure (AFM imaging of the same SWNT region with increasing compressive forces) is quite simple, fast, and precise, allowing accurate monitoring of the deformation process. In addition, from an extension of the developed theory and the definition of Young's modulus, it was found that the radial Young's modulus is not a constant for a given SWNT, but, rather, it is dependent on nanotube strain, explaining the wide variation for this parameter found in the literature. Finally, possible implications of the present work to the nanometrology field were discussed, suggesting a formal relationship between the applied force, SWNT diameter, and AFM tip radius, which enables accurate determination of one of them if the other two are precisely known.

We would like to thank A. S. Ferlauto for the sample growth, A. P. Gomes and M. A. Pimenta for the Raman characterization of the sample, and M. S. C. Mazzoni for helpful discussions. Financial support from Fapemig, Capes, CNPq, Instituto de Nanotecnologia/MCT and Rede Nacional de Pesquisas em Nanotubos de Carbono are also acknowledged.

*chacham@fisica.ufmg.br
†bernardo@fisica.ufmg.br

[1] A. Jorio, M. S. Dresselhaus, and G. Dresselhaus, *Carbon Nanotubes: Advanced Topics in Synthesis, Properties and Applications*, Topics in Applied Physics Vol. 111 (Springer, Berlin, 2007).
[2] G. Gao, T. Cagin, and W. A. Goddard III, Nanotechnology **9**, 184 (1998).
[3] B. Vigolo *et al.*, Science **290**, 1331 (2000).
[4] A. B. Dalton *et al.*, Nature (London) **423**, 703 (2003).
[5] P. J. de Pablo *et al.*, Phys. Rev. Lett. **91**, 098101 (2003).
[6] L. M. Ericson *et al.*, Science **305**, 1447 (2004).
[7] J. A. Elliott *et al.*, Phys. Rev. Lett. **92**, 095501 (2004).
[8] D. Y. Sun *et al.*, Phys. Rev. B **70**, 165417 (2004).
[9] I. Palaci *et al.*, Phys. Rev. Lett. **94**, 175502 (2005).
[10] H.-Y. Wang *et al.*, Appl. Phys. Lett. **89**, 211906 (2006).
[11] M. Hasegawa and K. Nishidate, Phys. Rev. B **74**, 115401 (2006).
[12] M. Minary-Jolandan and M.-F. Yua, J. Appl. Phys. **103**, 073516 (2008).
[13] S. Reich, C. Thomsen, and P. Ordejon, Phys. Rev. B **65**, 153407 (2002).
[14] T. W. Tombler *et al.*, Nature (London) **405**, 769 (2000).
[15] W. Shen *et al.*, Phys. Rev. Lett. **84**, 3634 (2000).
[16] C. Gomez-Navarro, P. J. Pablo, and J. Gómez-Herrero, Adv. Mater. **16**, 549 (2004).
[17] L. Vitali *et al.*, Phys. Rev. Lett. **96**, 086804 (2006).
[18] A. P. M. Barboza *et al.*, Phys. Rev. Lett. **100**, 256804 (2008).
[19] J. Kong, A. M. Cassell, and H. Dai, Chem. Phys. Lett. **292**, 567 (1998). Further sample characterization was carried out via resonant Raman spectroscopy of almost a hundred nanotubes, which were all found to be isolated single-wall carbon nanotubes [30].
[20] J. E. Sader, J. W. M. Chon, and P. Mulvaney, Rev. Sci. Instrum. **70**, 3967 (1999).
[21] D. A. Bonnell, *Scanning Probe Microscopy and Spectroscopy* (Wiley-VCH, New York, 2001).
[22] In order to quantify the absolute deformation $(d - h)$ and, then, the radial strain $[s = (d - h)/d]$ of each SWNT, its original diameter d (or height h for zero compressive force) must be estimated. Therefore, using the experimental data in Fig. 1(b), the value of d was estimated for each SWNT simply through linear extrapolation of the measured h to $F = 0$.
[23] A. P. Boresi and O. M. Sidebottom, *Advanced Mechanics of Materials* (John Wiley & Sons, New York, 1993).
[24] M. S. C. Mazzoni and H. Chacham, Appl. Phys. Lett. **76**, 1561 (2000).
[25] The model therefore neglects tip-nanotube interactions for $y > d$. From tip-sample attractive force measurements, we estimate that this would lead to corrections smaller than 1.5 nN. For very large forces, such that opposite tube walls are at distances smaller than 0.4 nm, wall-to-wall interactions [26,27] will be relevant. However, only a few points on Fig. 1(b) are near that distance range.
[26] W. Guo *et al.*, Phys. Rev. Lett. **93**, 245502 (2004).
[27] T. Chang *et al.*, Appl. Phys. Lett. **88**, 211906 (2006).
[28] T. DeBorde *et al.*, Nano Lett. **8**, 3568 (2008).
[29] Following the same model described in the inset of Fig. 1(b), the AFM tip-SWNT contact area A can be calculated as a function of strain s, resulting in $A(s) = 5\pi\sqrt{2Rd^3s^3}/6$.
[30] A. P. Gomes and M. A. Pimenta (private communication).